

Oxidative Conversion of a Europium(II)-Based T_1 Agent into a Europium(III)-Based paraCEST Agent that can be Detected In Vivo by Magnetic Resonance Imaging

Alexander M. Funk, Veronica Clavijo Jordan, A. Dean Sherry, S. James Ratnakar,* and Zoltan Kovacs*

Abstract: The Eu^{II} complex of 1,4,7,10-tetraazacyclododecane-1,4,7,10-tetraacetic acid (DOTA) tetra(glycinate) has a higher reduction potential than most Eu^{II} chelates reported to date. The reduced Eu^{II} form acts as an efficient water proton T_1 relaxation reagent, while the Eu^{III} form acts as a water-based chemical exchange saturation transfer (CEST) agent. The complex has extremely fast water exchange rate. Oxidation to the corresponding Eu^{III} complex yields a well-defined signal from the paraCEST agent. The time course of oxidation was studied in vitro and in vivo by T_1 -weighted and CEST imaging.

Gadolinium complexes are commonly used as contrast agents in magnetic resonance imaging (MRI). They generate image contrast by shortening the longitudinal (T_1) relaxation time of bulk water protons. The efficiency of a T_1 agent is defined by r_1 relaxivity, which is dependent on several parameters, including the metal bound water exchange rate, rotational correlation time of the complex, and the electronic relaxation time of the metal ion.^[1] An alternative to the Gd^{3+} -based contrast agents is the isoelectronic Eu^{2+} ion.^[2] Both ions have a $4f^7$ electron configuration and a symmetric $^8S_{7/2}$ ground state but Eu^{2+} complexes in general display much faster water exchange rates and faster electronic relaxation times.^[2] Analogous complexes of Eu^{2+} and Gd^{3+} can produce similar relaxivity values at lower fields while at higher fields the Eu^{2+} complexes tend to be more efficient.^[3]

The Eu^{2+} aqua ion is extremely sensitive to oxidation as demonstrated by its strongly negative reduction potential (-585 mV vs. Ag^+/AgCl). Eu^{2+} poly(amino carboxylate) chelates usually have lower reduction potential, although some Eu^{2+} cryptates have been reported to be more stable towards oxidation.^[4,5] Eu^{2+} complexes have been proposed as redox sensitive T_1 agents,^[3,5,6] because oxidation of Eu^{2+} leads to the formation of weakly paramagnetic Eu^{3+} , which has little impact on water proton T_1 . The Eu^{3+} ion however

generates a moderately strong magnetic dipolar field that produces large hyperfine shifts of NMR signals of nearby ligand protons. While Eu^{3+} complexes are very poor T_1 -shortening agents, Eu^{3+} DOTA tetra(amides) (Figure 1)

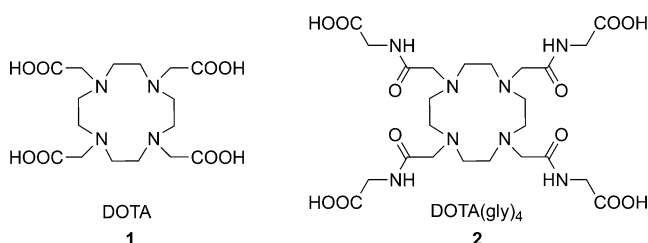


Figure 1. Structure of 1,4,7,10-tetraazacyclododecane-1,4,7,10-tetraacetic acid **1** and 1,4,7,10-tetraazacyclododecane-1,4,7,10-tetraacetic acid tetra(glycine amide) **2**.

belong to a conceptually different class of MRI contrast agents, known as paraCEST agents that alter image contrast by transferring selectively saturated spins from a highly shifted small pool of proton spins (metal-bound water) to the bulk water pool.^[7] Chemical exchange saturation transfer (CEST) occurs when the proton exchange rate between the two pools (k_{ex}) is in the slow-to-intermediate exchange regime ($k_{\text{ex}} \leq \Delta\omega$, where $\Delta\omega$ is the chemical shift difference between the two pools). A redox responsive liposomal $\text{Eu}^{2+}/\text{Eu}^{3+}$ system was recently reported that showed T_1 shortening effect and lipoCEST effect ($\Delta\omega \approx 1$ ppm) originating from the exchange between the water protons inside the liposomes and the bulk water protons not associated with the liposomes. Upon oxidation, the T_1 enhancement disappeared while the lipoCEST remained unaffected. The CEST effect in this system is not due to the formation of a Eu^{3+} complex.^[8]

Eu^{2+} complexes have several orders of magnitude faster water exchange rates in comparison to the corresponding Eu^{3+} complexes and with a suitable ligand system, may offer a unique opportunity in the design of redox responsive MR agent that shortens T_1 in the reduced state and produces a CEST signal in the oxidized state. In the present work we show that $\text{Eu}^{2+}\mathbf{2}$ is an efficient T_1 shortening agent because of the rapid water exchange of the Eu^{2+} bound water, but upon oxidation it turns into the well-known paraCEST agent, $\text{Eu}^{3+}\mathbf{2}$, which has slow water exchange kinetics. Merbach suggested in 2003 that the redox stability of $\text{Eu}^{2+}\mathbf{1}$ could be increased by substituting nitrogen containing donor groups for the carboxylate side-arms.^[3,6] Here, we also show that

[*] Dr. A. M. Funk, Dr. V. Clavijo Jordan, Prof. A. D. Sherry, Dr. S. J. Ratnakar, Prof. Z. Kovacs
Advanced Imaging Research Center
UT Southwestern Medical Center
5323 Harry Hines Blvd, Dallas, TX 75390 (USA)
E-mail: james.ratnakar@utsouthwestern.edu
zoltan.kovacs@utsouthwestern.edu

Prof. A. D. Sherry

Department of Chemistry, University of Texas, Dallas
800 West Campbell Road, Richardson, TX 75080 (USA)

Supporting information for this article can be found under:
<http://dx.doi.org/10.1002/anie.201511649>.

$\text{Eu}^{2+}\mathbf{2}$ indeed has significantly improved redox stability compared to $\text{Eu}^{2+}\mathbf{1}$.

The CEST effect can be expressed as a decrease in total bulk water signal intensity, and assuming complete and instantaneous saturation of the bound water peak, the net magnetization of water protons at steady-state is given by the following equation:

$$\text{CEST effect (\%)} = 1 - \left(\frac{M_s}{M_0} \right) = 100 \left(1 + \frac{cqT_1}{111\tau_M} \right)^{-1} \quad (1)$$

where c is the concentration of the agent, q is the number of protons per agent, 111 represents the molar concentration of bulk water protons, T_1 is the longitudinal (spin-lattice) relaxation time of bulk water, and τ_M is the lifetime of the exchanging proton ($\tau_M = 1/k_{\text{ex}}$).^[7] Thus, the magnitude of the CEST effect is dependent on both the agent concentration and the bulk water T_1 . Obviously, as $\text{Eu}^{2+}\mathbf{2}$ are oxidized, the T_1 shortening effect of Eu^{2+} will diminish while the paraCEST agent concentration will increase over the course of the reaction. To study the dependence of CEST on T_1 , we designed a model experiment in which the paraCEST agent $\text{Eu}^{3+}\mathbf{2}$ were mixed with varying concentration of the T_1 shortening agent $\text{Gd}^{3+}\mathbf{1}$ (Supporting Information, Table S1). Figure 2 shows that the proton relaxation rate ($R_1 = 1/T_1$) of bulk water protons increases with increasing $[\text{Gd}^{3+}\mathbf{1}]$ while the CEST signal from the paraCEST agent diminishes. At the two extremes of $[\text{Gd}^{3+}\mathbf{1}]$, the images are dominated by either CEST (when $[\text{Gd}^{3+}\mathbf{1}] = 0$) or T_1 (when $[\text{Gd}^{3+}\mathbf{1}] = 4 \text{ mM}$) but

there is a range of Gd^{3+} concentrations (samples 4, 5, and 6) where both CEST and T_1 enhancement contribute to the signal. The CEST signal was $< 10\%$ when $R_1 = 5 \text{ s}^{-1}$. From the fitting of the T_1 and CEST intensities to Equation (1), a bound water residence lifetime (τ_M) of 410 ms was obtained for $\text{Eu}^{3+}\mathbf{2}$ at 19°C , in agreement with the τ_M value determined by other methods.^[9] This same phenomenon, the sensitivity of CEST to water proton T_1 , formed the basis of a recently reported redox-sensitive paraCEST agent.

Eu^{2+} complexes of **1** and **2** were conveniently prepared by directly reacting the ligands with commercially available EuCl_2 under oxygen free conditions.^[10] The relaxivity of $\text{Eu}^{2+}\mathbf{2}$ was measured as $3.2 \text{ mM}^{-1} \text{ s}^{-1}$ at 9.4 T and 1 T (Supporting Information, Figures S1 and S2). The Eu^{2+} bound water exchange rate as estimated by fits of variable temperature ^{17}O NMR water linewidth data to theory was $k_{\text{ex}} = 0.21 \times 10^9 \text{ s}^{-1}$ for $\text{Eu}^{2+}\mathbf{2}$ and $k_{\text{ex}} = 0.63 \times 10^9 \text{ s}^{-1}$ for $\text{Eu}^{2+}\mathbf{1}$ in 20 % dioxane – 80 % water solutions (Supporting Information, Figures S3, S4 and Tables S2–S4), which are in the range of previously reported values.^[3,6,11,12] It is worth noting that the water exchange for $\text{Eu}^{2+}\mathbf{2}$ is nearly the same as that of $\text{Eu}^{2+}\mathbf{1}$. This indicates that the glycinate amide side-chains in $\text{Eu}^{2+}\mathbf{2}$ do not affect the water exchange rate in comparison to the corresponding Eu^{3+} complexes where the difference between carboxylate and amide donor ligands is typically three orders of magnitude.^[1,2] Unlike Gd^{3+} complexes, the r_1 value of $\text{Eu}^{2+}\mathbf{2}$ did not decrease significantly at high field, in agreement with previously published data for other Eu^{2+} complexes. The redox stability of $\text{Eu}^{2+}\mathbf{2}$ was studied by cyclic voltammetry. The reduction potential measured for the $\text{Eu}^{2+}\mathbf{2}/\text{Eu}^{3+}\mathbf{2}$ redox couple was found to be -226 mV vs. Ag^+/AgCl electrode (Supporting Information, Figure S5), which is far less negative than that of $\text{Eu}^{2+}\mathbf{1}$ (-1135 mV), or than the Eu^{2+} aqua ion (-585 mV against Ag^+/AgCl electrode).^[3] The rates of conversion of $\text{Eu}^{2+}\mathbf{2}$ and $\text{Eu}^{2+}\mathbf{1}$ to their respective Eu^{3+} complexes were also investigated by NMR by measuring the decay of the relaxation rate of the bulk water in a sealed NMR tube under N_2 atmosphere at 9.4 T (Supporting Information, Figures S6 and S7). The measured half-lives ($t_{1/2}$), 19 and 7 days, respectively, also show that $\text{Eu}^{2+}\mathbf{2}$ is the most stable cyclen-based Eu^{2+} complex reported so far. Similar stabilizing effect of the charge neutral amide group was reported for Eu^{2+} complexes of 1,10-diaza-18-crown-6 derivatives in which picolinamide pendant arms were substituted for picolinate groups.^[13]

Next, a fresh solution of $\text{Eu}^{2+}\mathbf{2}$ was prepared in a 6 mm tall vessel and exposed to air while both T_1 and CEST were measured as a function of time by imaging a slice 4 mm below the surface of the sample (Figure 3). As shown, the bulk water R_1 decreased steadily for about 100 minutes in this slice reflecting oxidation of Eu^{2+} to Eu^{3+} . The CEST signal increased following a sigmoid curve with an inflection point at around 100 min reaching 10% at around 6 s^{-1} bulk water relaxation rate in agreement with the results shown in Figure 2. These data reveal that relaxation of bulk water protons limits the intensity of the CEST signal and at about 80 min, the T_1 relaxation is slow enough for CEST to become efficient. As expected, the rate of oxidation depends heavily on the slice selected. For example, the T_1 enhancement in

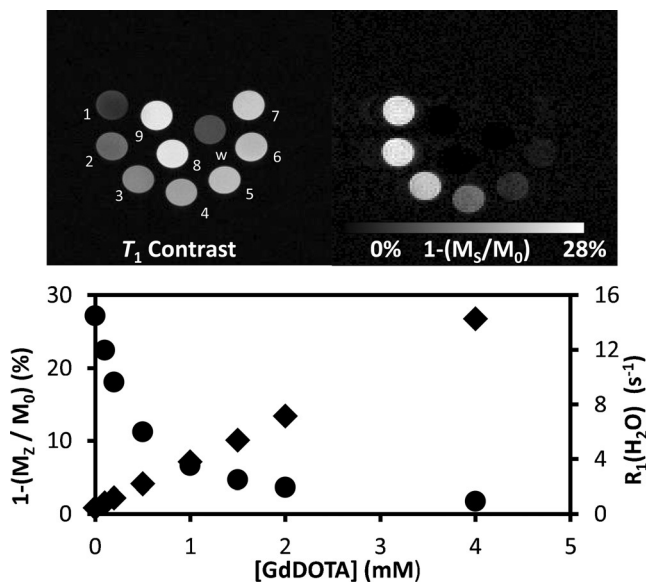


Figure 2. Top: Correlation between relaxation rates (♦) and the CEST effect (●) in a mixture of $\text{Gd}^{3+}\mathbf{1}$ and $\text{Eu}^{3+}\mathbf{2}$. Each circle in the image represents a separate sample. $[\text{Eu}^{3+}\mathbf{2}]$ in each sample was 10 mM while $[\text{Gd}^{3+}\mathbf{1}]$ ranged from 0 to 4 mM. Vial 9 contained 8 mM $\text{Gd}^{3+}\mathbf{1}$ alone while vial w contained only water. Bottom: Plots of CEST ($1-(M_s/M_0)$) and R_1 versus $[\text{Gd}^{3+}\mathbf{1}]$. Imaging parameters: $B_0 = 9.4 \text{ T}$, 20°C ; T_1 w: GEMS sequence, $\text{TR} = 9.9 \text{ ms}$, $\text{TE} = 5.0 \text{ ms}$; CEST: FSEMS sequence, sat time = 3 s, sat power = 10 μT , sat freq = 54 (on), –54 ppm (off-resonance).

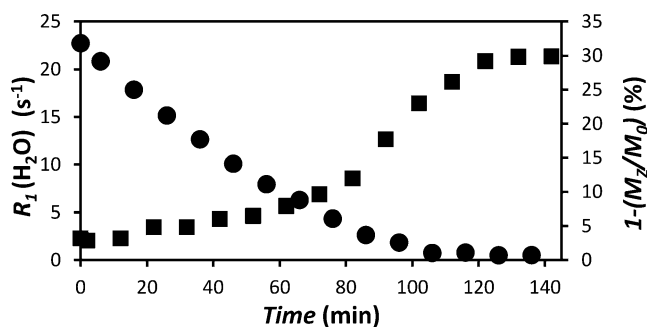


Figure 3. Plots of relaxation rate (R_1) (●) and CEST (■) for a solution initially containing 10 mM $\text{Eu}^{2+}2$ versus time. The data were collected from images in a single slice 4 mm away from the surface. Imaging parameters: $B_0 = 9.4$ T, 20°C , $T_1\text{w}$: FSEMS sequence, $\text{TR} = 2$ s, $\text{TE} = 3.0$ ms; CEST: FSEMS sequence, sat time = 3 s, sat power = $10\ \mu\text{T}$, sat freq = 54 (on-resonance), -54 ppm (off-resonance).

a slice just below the surface disappeared just after 10 minutes (Supporting Information, Figure S8).

To demonstrate the feasibility of using $\text{Eu}^{2+}2$ as redox sensitive probe we studied its reaction with H_2O_2 . A closed phantom containing $\text{Eu}^{2+}2$ solution (1 mL, 10 mM) was constructed and a small volume (20 μL) of hydrogen peroxide solution (3 %) was injected into the container. $T_1\text{w}$ and CEST images were recorded consecutively over a period of 1 h. As anticipated, the complex reacted rapidly with H_2O_2 and the mixing and diffusion of H_2O_2 in the solution could sequentially be observed by both $T_1\text{w}$ and CEST imaging. These images also demonstrate that the complex is stable in both oxidation states and throughout the process of oxidation (Figure 4; Supporting Information, Figures S9, S10).

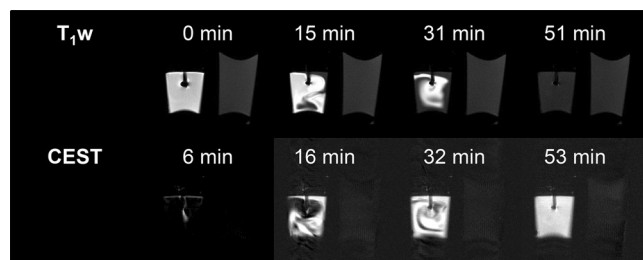


Figure 4. Sequential $T_1\text{w}$ (top) and CEST (bottom) images of a phantom containing $\text{Eu}^{2+}2$ (1 mL, 10 mM, left) and H_2O (right) after the injection of H_2O_2 (3 %, 20 μL). Imaging parameters: $B_0 = 9.4$ T, 20°C $T_1\text{w}$: FSEMS sequence, $\text{TR} = 2$ s, $\text{TE} = 5$ ms; PARACEST: FSEMS sequence, sat time = 3 s, sat power = $10\ \mu\text{T}$, sat freq = 54 (on-resonance), -54 ppm (off-resonance).

Encouraged by the enhanced stability of $\text{Eu}^{2+}2$ we tested the agent in vivo as well. The complex was injected into the thigh muscle of healthy male mice at a dose of $0.05\ \text{mmol kg}^{-1}$. Oxidation of the agent at the injection site could be observed by both $T_1\text{w}$ and CEST imaging (Figure 5). Given that diffusion of small molecules away from the injection site and into the vascular bed occurs relatively slowly, the relatively rapid decrease in water proton enhancement seen in $T_1\text{w}$ images at the injection site over ≈ 15 min presumably reflects oxidation of Eu^{2+} to Eu^{3+} . To validate this assump-

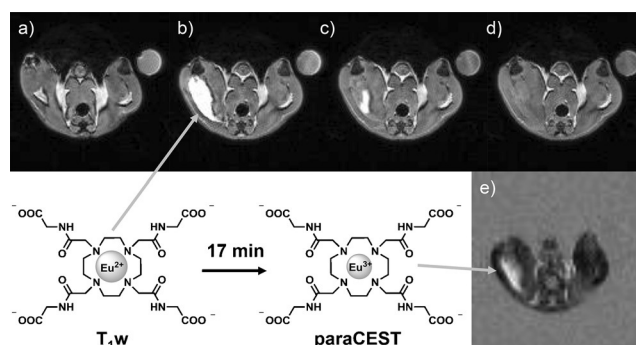


Figure 5. $T_1\text{w}$ and CEST imaging of an intramuscular injection of $\text{Eu}^{2+}2$ (10 mM, 100 μL) into the thigh muscle of a healthy male C57BL/6J mouse at $B_0 = 9.4$ T. $T_1\text{w}$ images at a) pre-injection, b) 5 min, c) 12 min, d) 16 min and e) the CEST image at 17 min. Selected imaging parameters: $T_1\text{w}$: ge3D sequence, $\text{TR} = 3.6$ ms, $\text{TE} = 1.8$ ms. $T_1\text{w}$ images have been normalized to muscle tissue; PARACEST: FSEMS sequence, sat time = 3 s, sat power = $10\ \mu\text{T}$, sat freq = 42 (on-resonance), -42 (off-resonance) ppm.

tion, after $T_1\text{w}$ enhancement of the signal vanished, CEST images were collected to verify that $\text{Eu}^{3+}2$ was indeed present. The CEST signal detected near the injection site (Figure 5e) remained evident over a period of about 20 min before disappearing (Supporting Information, Figure S11).

Since free Eu^{3+} does not produce a CEST effect, the detection of the agent by CEST imaging after the $T_1\text{w}$ enhancement indicates that the complex remained intact in vivo throughout the oxidation process. All of the mice recovered after imaging and no evidence of toxicity was apparent after injection of $\text{Eu}^{2+}2$.

In conclusion, we have shown that ligand **2** forms a complex with Eu^{2+} that is surprisingly stable to oxidation. The Eu^{2+} -bound water exchange rate for this complex ($k_{\text{ex}} = 0.21 \times 10^9\ \text{s}^{-1}$) was found to be extremely fast, indicating that the amide side-arms do not have a significant decelerating effect on the water exchange. The agent has different contrast enhancing properties depending on the oxidation state of the metal. In its divalent form it is an efficient T_1 shortening agent with an r_1 relaxivity comparable to Gd-based contrast agents. Oxidation converts it into $\text{Eu}^{3+}2$, which is a commonly used paramagnetic chemical exchange saturation (paraCEST) agent. The oxidation of $\text{Eu}^{2+}2$ by air or H_2O_2 could be followed by both $T_1\text{w}$ and CEST imaging. The improved oxidative stability of $\text{Eu}^{2+}2$ When injected intramuscularly into healthy mice the complex generated strong T_1 enhancement that gradually diminished over several minutes after which strong CEST effect could be observed at the injection site. This complex could serve as a design platform for a novel class of redox sensitive bimodal MR contrast agents in which the redox potential of the Eu^{2+} may be fine-tuned by the nature of the peripheral amide groups.

Acknowledgements

Financial support from the NIH (R01-CA115531, P41-EB015908 and 1P30-CA142543), CPRIT RP130362, and the Robert A. Welch Foundation (AT-584) is acknowledged. The

authors thank Prof Kayla Green (Texas Christian University) for help with cyclic voltammetry.

Keywords: contrast agents · divalent lanthanides · europium · paraCEST · T_1 weighting

How to cite: *Angew. Chem. Int. Ed.* **2016**, 55, 5118–5027
Angew. Chem. **2016**, 128, 5108–5111

-
- [1] P. Caravan, J. J. Ellison, T. J. McMurry, R. B. Lauffer, *Chem. Rev.* **1999**, 99, 2293–2352.
- [2] É. Tóth, L. Burai, A. E. Merbach, *Coord. Chem. Rev.* **2001**, 216–217, 363–382.
- [3] L. Burai, É. Tóth, G. Moreau, A. Sour, R. Scopelliti, A. E. Merbach, *Chem. Eur. J.* **2003**, 9, 1394–1404.
- [4] N.-D. H. Gamage, Y. Mei, J. Garcia, M. J. Allen, *Angew. Chem. Int. Ed.* **2010**, 49, 8923–8925; *Angew. Chem.* **2010**, 122, 9107–9109.
- [5] L. A. Ekanger, L. A. Polin, Y. Shen, E. M. Haacke, P. D. Martin, M. J. Allen, *Angew. Chem. Int. Ed.* **2015**, 54, 14398–14401; *Angew. Chem.* **2015**, 127, 14606–14609.
- [6] P. Caravan, A. E. Merbach, *Chem. Commun.* **1997**, 2147–2148.
- [7] S. Viswanathan, Z. Kovacs, K. N. Green, S. J. Ratnakar, A. D. Sherry, *Chem. Rev.* **2010**, 110, 2960–3018.
- [8] L. A. Ekanger, M. M. Ali, M. J. Allen, *Chem. Commun.* **2014**, 50, 14835–14838.
- [9] W. T. Dixon, J. Ren, A. J. M. Lubag, J. Ratnakar, E. Vinogradov, I. Hancu, R. E. Lenkinski, A. D. Sherry, *Magn. Reson. Med.* **2010**, 63, 625–632.
- [10] G. Zucchi, P. Thuéry, E. Rivière, M. Ephritikhine, *Chem. Commun.* **2010**, 46, 9143–9145.
- [11] G. Moreau, L. Burai, L. Helm, J. Purans, A. E. Merbach, *J. Phys. Chem. A* **2003**, 107, 758–769.
- [12] S. Seibig, É. Tóth, A. E. Merbach, *J. Am. Chem. Soc.* **2000**, 122, 5822–5830.
- [13] M. Regueiro-Figueroa, J. L. Barriada, A. Pallier, D. Esteban-Gómez, A. de Blas, T. Rodríguez-Blas, É. Tóth, C. Platas-Iglesias, *Inorg. Chem.* **2015**, 54, 4940–4952.

Received: December 15, 2015

Revised: January 22, 2016

Published online: March 8, 2016
